A Large Annual Cycle in Ozone above the Tropical Tropopause Linked to the Brewer–Dobson Circulation

WILLIAM J. RANDEL, MIJEONG PARK, AND FEI WU

National Center for Atmospheric Research, Boulder, Colorado*

NATHANIEL LIVESEY

Jet Propulsion Laboratory, California Institute of Technology, Pasadena, California

(Manuscript received 23 January 2007, in final form 19 March 2007)

ABSTRACT

Near-equatorial ozone observations from balloon and satellite measurements reveal a large annual cycle in ozone above the tropical tropopause. The relative amplitude of the annual cycle is large in a narrow vertical layer between ~16 and 19 km, with approximately a factor of 2 change in ozone between the minimum (during NH winter) and maximum (during NH summer). The annual cycle in ozone occurs over the same altitude region, and is approximately in phase with the well-known annual variation in tropical temperature. This study shows that the large annual variation in ozone occurs primarily because of variations in vertical transport associated with mean upwelling in the lower stratosphere (the Brewer–Dobson circulation); the maximum relative amplitude peak in the lower stratosphere is collocated with the strongest background vertical gradients in ozone. A similar large seasonal cycle is observed in carbon monoxide (CO) above the tropical tropopause, which is approximately out of phase with ozone (associated with an oppositely signed vertical gradient). The observed ozone and CO variations can be used to constrain estimates of the seasonal cycle in tropical upwelling.

1. Introduction

The seasonal variation of stratospheric ozone has been well documented based on satellite data (McCormick et al. 1989) and ozonesonde measurements (Logan 1999). One feature that has received relatively little attention (beyond a mention in Logan 1999) is the presence of a large annual cycle in ozone over a narrow region just above the tropical tropopause. This variability is evident in analysis of high vertical resolution ozonesonde data from the tropical Southern Hemisphere Additional Ozonesondes (SHADOZ) network (Thompson et al. 2003a,b). The large annual cycle near the tropopause was noted in Thompson et al. (2003b), who focused on tropospheric ozone, and Randel et al. (2006), who highlighted interannual changes in the SHADOZ data. Folkins et al. (2006a) have recently discussed the ozone seasonal cycle near the tropopause, focusing on coupling to the seasonal cycle in vertical circulation and convective outflow; they also discuss related variability in tropical carbon monoxide (CO). Our study is a complement to Folkins et al. (2006a), focusing on the role of tropical upwelling in driving the annual cycle in ozone (and CO), including the detailed vertical structure and relationships to temperature in the lower stratosphere.

Our analysis is organized as follows. We first present the detailed vertical and latitudinal structure of the ozone seasonal cycle based on ozonesonde and satellite data. We then demonstrate that the observed sharply peaked vertical structure is primarily a response to the annual cycle of upwelling acting on the strong background vertical gradient in ozone near and above the tropopause. This mechanism explains the close association between the ozone and temperature seasonal cycles in this region. We also explore the seasonal cycle

* The National Center for Atmospheric Research is sponsored by the National Science Foundation.

Corresponding author address: William Randel, National Center for Atmospheric Research, Boulder, CO 80307.
E-mail: randel@ucar.edu

DOI: 10.1175/2007JAS2409.1

in CO, and demonstrate that upwelling has a dominant influence on seasonality in the lower stratosphere. Because variations in the circulation are the dominant forcing mechanism above ~16 km, the ozone and CO observations can be used to provide independent estimates of the seasonal cycle in tropical upwelling (which is not well quantified in the lower stratosphere).

2. Data and analyses

Time series of tropical ozone profiles are obtained from the SHADOZ data archive (available online at http://croc.gsfc.nasa.gov/shadoz/; Thompson et al. 2003a). SHADOZ consists of a set of 12 tropical stations with ozonesonde soundings several times per month, beginning in 1998. The analyses here focus on data from 7 near-equatorial stations with dense data records covering 1998–2006. These stations include Nairobi, Kenya (1°S); Kuala Lumpur, Malaysia (3°N); San Cristobal Island (1°S); Ascension Island (8°S); Wautesok, Java (8°S); Malindi, Kenya (3°S); and Paramaribo, Suriname (6°N). The ozonesonde soundings also include temperature profile measurements, which we use to study the corresponding seasonal variation in temperatures. We also use a high vertical resolution global temperature climatology derived from Challenging Minisatellite Payload (CHAMP) GPS radio occultation measurements over 2001–06 (Wickert et al. 2001) as input to radiative heating calculations, used to estimate seasonal variations in tropical upwelling. This temperature climatology was derived from the CHAMP data using a harmonic seasonal cycle fit, as discussed in Randel et al. (2003). The upwelling calculations are described in detail in Randel et al. (2002).

We also include analysis of ozone observations from satellite data, to provide a global perspective. We include results from the Halogen Occultation Experiment (HALOE) covering 1992–2005 (Russell et al. 1993), and also from *Aura* Microwave Limb Sounder (MLS) observations covering 2004–06 (Waters et al. 2006). HALOE has the advantage of high vertical resolution (~2 km), but relatively few observations during individual months (a total of approximately 1000 observations over 10°N–S during 1992–2005). MLS ozone retrievals have somewhat lower vertical resolution (~3 km), but have the advantage of daily tropical observations. We also include analysis of MLS CO data, motivated by the analyses of Folkins et al. (2006a); these retrievals have somewhat lower effective vertical resolution of ~4.5 km. The MLS CO data are most useful for pressure levels 46, 68, 100, and 147 hPa, and we focus on these levels (note these are oversampled in the vertical, given the ~4.5-km vertical resolution of the retrieval).

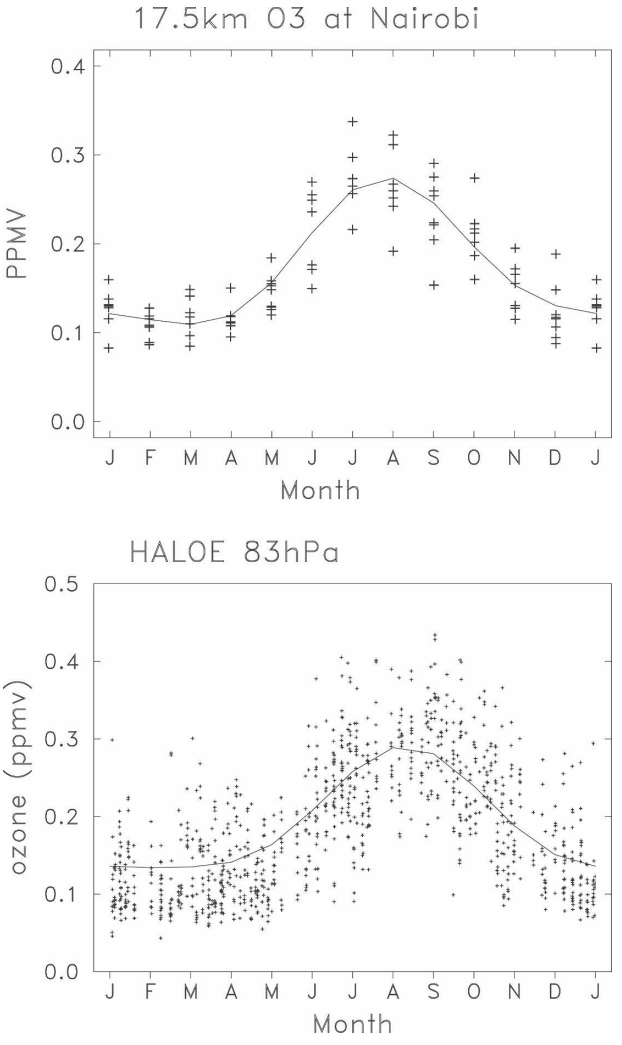

FIG. 1. (top) Ozone mixing ratio (ppmv) at 17.5 km derived from ozonesonde measurements over Nairobi during 1998–2006, plotted according to month of the observation. (bottom) HALOE ozone observations at 83 hPa over 10°N–S, combining all observations over 1992–2005. The thin line in each panel shows the harmonic seasonal cycle fit to the individual points.

3. Results

a. Seasonal cycle in ozone near the tropical tropopause

The observed seasonal cycle in ozone from SHADOZ data is characterized by combining observations from all years (1998–2006) to derive a composite seasonal cycle for each station. Figure 1a shows ozone measurements from Nairobi at 17.5 km, binned according to month, showing a large annual cycle varying from ~0.1 ppmv during NH winter to ~0.25 ppmv during NH summer. Figure 1b shows a corresponding plot of equatorial ozone variations at 83 hPa derived from

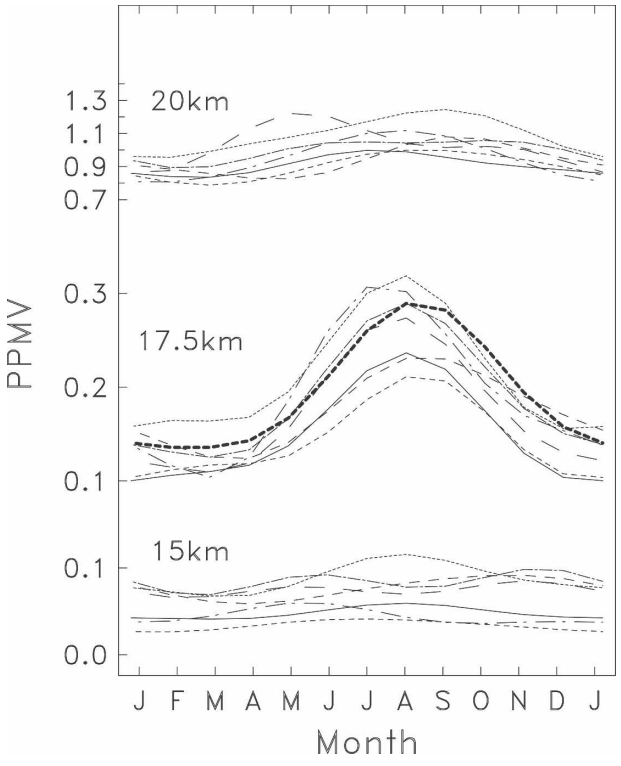

FIG. 2. Seasonal cycle fit of ozone mixing ratio (ppmv) at each of the SHADOZ stations at 15, 17.5, and 20 km. Each line represents the harmonic fit of the data at the individual stations. The heavy dashed line at 17.5 km is the corresponding result from HALOE data over 10°N–S.

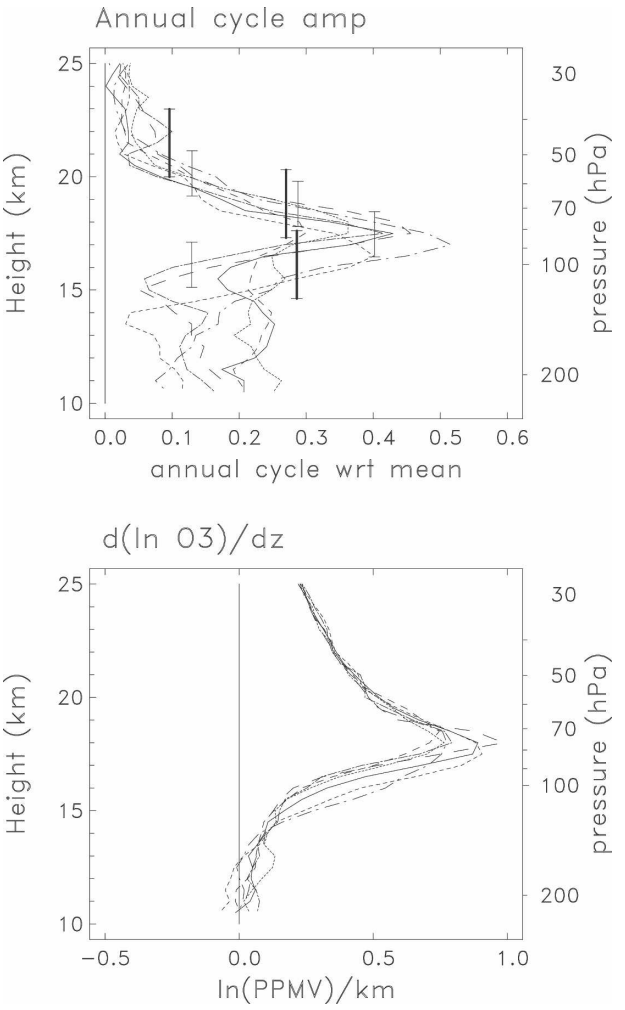

FIG. 3. (top) Vertical structure of the relative amplitude of the annual cycle in ozone at each of the SHADOZ stations. The annual cycle amplitude is calculated by a harmonic fit to the data at each station (same as in Fig. 1a), and normalized by the respective annual mean ozone at each level. Corresponding results are also shown for MLS and HALOE satellite data (wider and narrower vertical bars, respectively), and the vertical width of the symbols denotes the effective vertical averaging in the respective measurements. (bottom) Vertical structure of the quantity $d\ln(O_3)/dz$, calculated for annually averaged data at each SHADOZ station.

HALOE measurements, showing very similar variability. The thin lines in Figs. 1a,b show harmonic seasonal cycle fits to the monthly data, which we use to quantify the seasonal variation. Figure 2 shows the seasonal fit for each near-equatorial SHADOZ station, at 15, 17.5, and 20 km. At 17.5 km each station shows a similarly sized and approximately in-phase seasonal cycle; because the stations vary widely in longitude, this demonstrates that the annual cycle at 17.5 km is primarily a zonal mean feature (consistent with the HALOE data included in Fig. 2). Figure 2 furthermore shows that there are small annual cycles at 15 and 20 km, so that the large annual cycle is confined to a relatively narrow vertical layer.

The vertical structure of the tropical ozone annual cycle at each station is quantified in Fig. 3a, which shows the amplitude of the annual harmonic (A_1) normalized by the annual mean value $\langle A \rangle$ at each altitude. A well-defined maximum is observed for this ratio ($A_1/\langle A \rangle$) at each station, peaking with values of ~0.4, and extending over a narrow vertical range (~16–19 km). Note that a relative amplitude of 0.4 corresponds to a maximum–minimum ratio of approximately 2.4 over the seasonal cycle. Large variability in ozone annual cycle amplitude is observed among the different stations below ~15 km in Fig. 3a, and this reflects the longitudinal dependence of seasonal ozone variability in the tropical upper troposphere, as discussed in Thompson et al. (2003b). Above 20 km, Fig. 3a shows that the relative annual cycle amplitude is very small.

Figure 3a also includes the relative annual cycle amplitude for ozone derived from HALOE and MLS satellite data. The structure derived from HALOE data agrees reasonably well with the ozonesonde profiles,

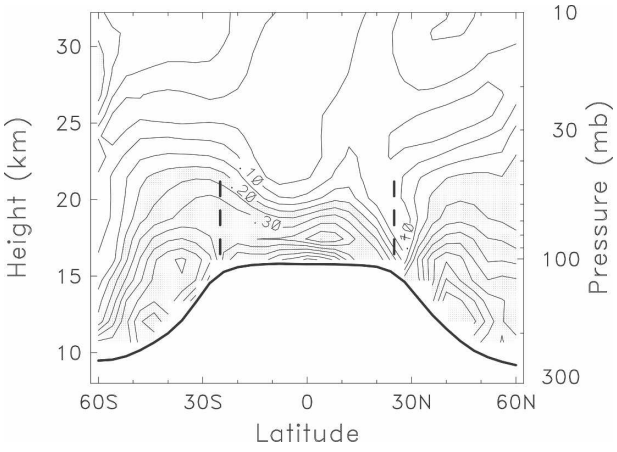

FIG. 4. Meridional cross section of the relative amplitude of the ozone seasonal cycle derived from HALOE data. Contour interval is 0.05. The continuous heavy line denotes the tropopause, and the vertical dashed lines near 25°N–S indicate the latitude range of mean tropical upwelling.

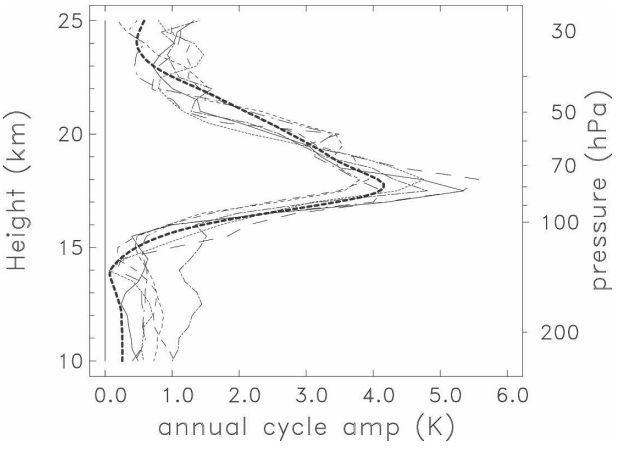

FIG. 5. Vertical structure of the annual cycle amplitude in tropical temperatures, derived from radiosonde measurements at each SHADOZ station. The heavy dashed line shows a corresponding result derived from the zonal average GPS temperature climatology.

with a clear maximum at the 83-hPa level. The MLS data do not resolve the strong peak near 17.5 km, but agree reasonably well with the ozonesonde and HALOE results at 100 and 68 hPa (given the ~3 km vertical resolution of MLS). These comparisons demonstrate the need for high vertical resolution measurements to adequately resolve the seasonal cycle above the tropopause.

A near-global view of the normalized annual cycle amplitude ($A_1/\langle A\rangle$) for ozone derived from zonally averaged HALOE data is shown in Fig. 4. A narrow maximum is evident above the tropical tropopause, with vertical structure very similar to the average ozonesonde results (as shown by the HALOE data points in Fig. 3a). The HALOE data help define the latitudinal structure of this maximum, showing largest amplitude over ~15°N–15°S. Relatively large annual variations in ozone are also evident in the extratropical lower stratosphere of both hemispheres in Fig. 4, and these are associated with the well-known winter–spring maxima and summer minima in each hemisphere (e.g., Pan et al. 1997). There is approximately a 6-month phase shift between the annual ozone maximum in the Tropics and that in the NH (and a corresponding annual amplitude minimum near 25°N seen in Fig. 4), whereas there is a relatively small phase shift (~1 month) between the Tropics and SH midlatitudes. However, the tropical annual cycle is probably a distinct phenomenon, as it has a characteristic vertical structure that is distinct from that in SH midlatitudes. The overall latitudinal structure of the tropical maximum is consistent with the width of the tropical upwelling region, ~25°N–S (Rosenlof 1995).

b. *Associations with the seasonal cycle in tropical upwelling*

A large annual cycle in temperature near the tropical tropopause is a well-known feature of the general circulation (Reed and Vlcek 1969; Yulaeva et al. 1994), and this is primarily associated with an annual cycle in vertical velocity (tropical upwelling). Figure 5 shows the amplitude of the annual cycle in temperature derived from radiosonde measurements at each of the SHADOZ stations (sampled identically to ozone), highlighting a sharply peaked maximum over ~16–21 km. Figure 5 also includes results for zonal mean temperature over 10°N–S derived from GPS radio occultation measurements (as in Randel et al. 2003), showing a very similar vertical structure. The vertical profile of the temperature annual cycle is very similar to that for ozone (Fig. 3a), and the two oscillations are nearly in phase (Fig. 6), suggesting a similar forcing mechanism. The annual cycle in tropical temperatures is reasonably well understood to result from the annual variation in tropical upwelling (Yulaeva et al. 1994), which in turn is driven by wave forcing from the middle and/or low latitudes (Rosenlof 1995; Plumb and Eluszkiewicz 1999; Randel et al. 2002; Kerr-Munslow and Norton 2006). The approximate thermodynamic balance in this region, assuming a linear relaxational approximation for radiative heating, can be written as (Randel et al. 2002)

$$\frac{\partial \overline{T}}{\partial t} + \overline{w}^{*} S = -\alpha_r(\overline{T} - \overline{T}_e). \quad (1)$$

Here $\overline{T}$ is zonal mean temperature, $\overline{w}^{*}$ the vertical velocity, S a static stability parameter, α_r an inverse ra-

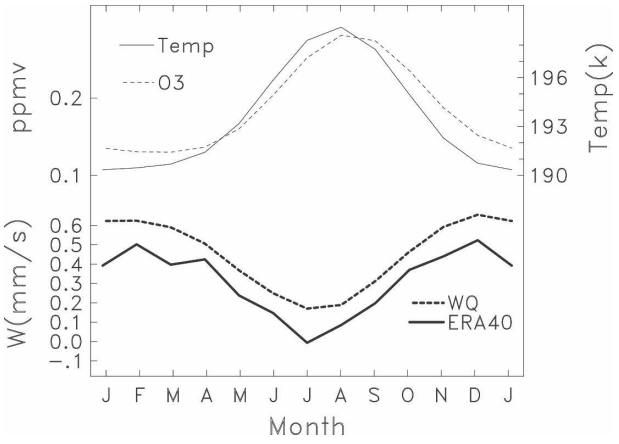

FIG. 6. Time series of temperature, ozone, and upwelling in the Tropics near 17.5 km. Temperature is from the GPS climatology, and ozone is the average from all of the SHADOZ stations. Upwelling (w^*_Q) is calculated from thermodynamic balance, incorporating GPS temperatures and an accurate radiative transfer scheme. Also shown is upwelling estimated from the ERA-40 reanalysis.

diative damping time scale, and $\overline{T}_e$ the radiative equilibrium temperature. The enhanced amplitude of the temperature annual cycle near and above the tropopause seen in Fig. 5 is attributable to the very long radiative damping time scales (small α_r) in the lower stratosphere (Randel et al. 2002). Figure 6 shows the zonal mean vertical velocity at 17.5 km over 15°N–S estimated from thermodynamic balance, using an accurate radiative transfer scheme (including seasonally varying ozone) to calculate heating rates. For comparison we also include zonal mean $\overline{w}^*$ derived from 40-yr European Centre for Medium-Range Weather Forecasts (ECMWF) Re-Analysis (ERA-40) (Uppala et al. 2005), and this shows reasonable agreement with the thermodynamic balance estimate, especially regarding the seasonal cycle. The similarity in behavior of ozone and temperature in Fig. 6, together with the fact that both ozone and (potential) temperature have strong positive vertical gradients in the lower stratosphere, suggests that the ozone seasonal cycle may also result primarily from the annual cycle in upwelling. We attempt to quantify this relationship below.

The zonal average continuity equation for ozone mixing ratio ($\overline{x}$) can be written as [Andrews et al. 1987, their Eq. (9.4.13)]

$$\frac{\partial \overline{x}}{\partial t} + \overline{v}^* \overline{x}_y + \overline{w}^* \overline{x}_z = \nabla \cdot \mathbf{M} + P - L. \qquad (2)$$

Here $\overline{v}^*$ and $\overline{w}^*$ are components of the residual mean circulation, $\nabla \cdot \mathbf{M}$ is an eddy transport term, and $P - L$ represents chemical production minus loss. We focus on variability associated with the seasonal cycle, and separate the terms according to the annual average and harmonic annual variations as $\overline{\chi} = \langle \overline{\chi} \rangle + \chi_1 e^{i\sigma t}$, with $\sigma = 2\pi/(365 \text{ days})$ [and likewise for each term in (2)]. For the region near the tropical tropopause, we neglect the v^* term (because of very small meridional ozone gradients in this region), and the $P - L$ terms (we assume there is an insignificant annual cycle in photochemical ozone production, because the solar zenith angle has a semiannual variation over the equator). We also neglect the $\nabla \cdot \mathbf{M}$ term in (2), which represents eddy transport into and out of the Tropics. While such eddy transports are likely to be important for the ozone balance in the Tropics (Avalone and Prather 1996; Volk et al. 1996), for simplicity we assume that this contribution does not have a large systematic annual variation (this is a limitation to this analysis, as discussed below). The resulting balance for the seasonal variations (terms proportional to $e^{i\sigma t}$) from (2) is then

$$i\sigma \overline{\chi}_1 + \overline{w}^*_1 \langle \overline{\chi}_z \rangle = 0. \qquad (3)$$

In other words, the annual cycle in $\overline{x}$ is primarily driven by the variation in vertical velocity acting on the background vertical gradient $\langle \overline{\chi}_z \rangle$. In getting to Eq. (3), we have neglected a term $\langle \overline{w^*} \rangle \overline{\chi}_{1z}$, which is small. To analyze fractional ozone variations, we divide by the annual average ozone, giving

$$\frac{1}{\langle \overline{\chi} \rangle} i\sigma \overline{\chi}_1 + \overline{w}^*_1 \frac{\langle \overline{\chi}_z \rangle}{\langle \overline{\chi} \rangle} = 0. \qquad (4)$$

Relabeling the zonal mean ozone $\overline{\chi} = A$ and $\langle \overline{w^*_1} \rangle$ as w_1, the approximate fractional continuity Eq. (4) is

$$i\sigma \frac{A_1}{\langle A \rangle} + w_1 \frac{\partial \ln \langle A \rangle}{\partial z} = 0. \qquad (5)$$

Equation (5) relates the fractional ozone annual cycle amplitude ($A_1/\langle A \rangle$) to the annual cycle in upwelling (w_1), multiplied by the factor ($\partial \ln \langle A \rangle / \partial z$). Figure 3b shows this latter quantity calculated from the annual average SHADOZ data, and this highlights a strong maximum in the lower stratosphere, with a very similar vertical structure as the maximum in annual cycle amplitude (Fig. 3a). This similar vertical structure suggests that the approximate balance in Eq. (5) is reasonable, and provides a simple physical mechanism for the location and narrow vertical structure of the ozone annual cycle (namely, it is due to the strongest vertical gradients in background ozone).

Given the observed seasonal cycle and background ozone structure from the SHADOZ data (Figs. 3a,b), the approximate balance in Eq. (5) can be used to estimate the annual cycle amplitude in vertical velocity (w_1). Figure 7 shows the vertical profile of w_1 calculated

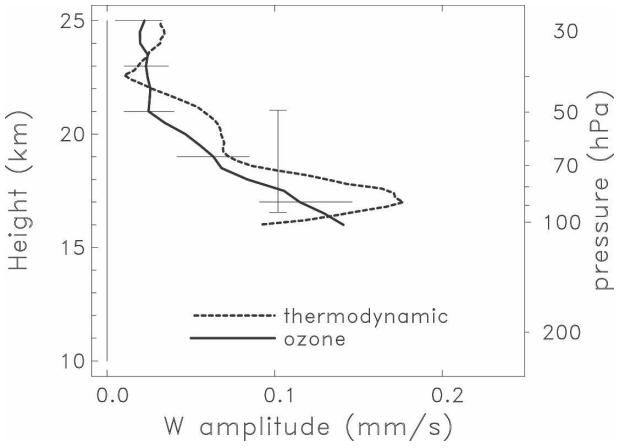

FIG. 7. Vertical structure of the annual cycle amplitude in tropical upwelling (w_1). Dashed line shows results derived using vertical velocity fields estimated from thermodynamic balance. Solid line shows the result estimated from the observed annual cycle in ozone using Eq. (5), from measurements at the SHADOZ stations. Error bars on the ozone curve shows the range of results among the 7 individual stations. The vertical bar shows the estimate of w_1 derived from MLS CO data at 68 hPa, with details as discussed in the text.

in this manner from the SHADOZ data, by first averaging the $(A_1/\langle A\rangle)$ and $(\partial \ln\langle A\rangle/\partial z)$ over the individual stations (the range of results from the individual stations is also shown, giving an estimate of uncertainty). Figure 7 includes a comparison with the vertical structure of w_1 derived from thermodynamic balance. Overall there is quite reasonable agreement in the magnitude and vertical structure, with both estimates showing largest values near 100 hPa, and an overall decrease with altitude in the lower stratosphere. Note there is a maximum in w_1 amplitude near 17 km in the thermodynamic estimate that is not observed in the ozone results, but this difference is probably within uncertainty levels for both estimates [the radiative heating calculations do not include the effects of cirrus or deep convective clouds, which could be important near and above the tropopause (Corti et al. 2006; Fueglistaler and Fu 2006), and the ozone results are based on the simplified balance in Eq. (5)].

c. Seasonal cycle in tropical carbon monoxide

Folkins et al. (2006a) have highlighted a seasonal cycle in tropical CO, and we examine this variability and the links to tropical upwelling using the MLS data. Figure 8 shows time series of MLS CO at 147, 100, and 68 hPa over 10°S–20°N for the first 2 years of data (2004–2006). The CO data at 147 hPa show a predominant semiannual variation, probably linked to the seasonal cycle of biomass burning CO emissions in the Tropics lofted by deep convection (Folkins et al. 2006a; Schoeberl et al. 2006). At 68 hPa, CO exhibits a strong annual cycle (more than twice as large as at 147 hPa), and this CO annual cycle is approximately out of phase with ozone at this level (as shown using 68-hPa MLS ozone in Fig. 8). The phase of the CO annual cycle at 68 hPa lags the annual cycle in ozone by slightly more than 6 months (~7 months), but this might be expected as a result of the respective chemical lifetimes (see below). In addition to the dominant annual cycle variations, the time series in Fig. 8 show anticorrelated CO–ozone variability on shorter time scales (such as during January–February 2005), which may be evidence of shorter-term variability in tropical upwelling (as observed in temperatures, e.g., Randel et al. 2002). Seasonal variations of CO at 100 hPa in Fig. 8 show a behavior midway between the semiannual variation at 147 hPa and the dominant annual harmonic at 68 hPa. It is important to note the increase in (absolute) annual cycle amplitude between 147 and 68 hPa in Fig. 8, which implies that the annual variation at 68 hPa is not simply a result of vertical advection of the signal below the tropopause.

The simplified tracer continuity equation for CO in the tropical lower stratosphere can be written as

$$i\sigma\bar{\chi}_1 + \overline{w_1^*\langle\bar{\chi}_z\rangle} = -\alpha_c\bar{\chi}_1. \quad (6)$$

This is similar to Eq. (4), but with an additional term on the right-hand side that represents chemical relaxation, parameterized by an inverse chemical lifetime α_c. An approximate damping time scale for CO in the tropical lower stratosphere is ~4 months (J.-F. Lamarque 2006, personal communication; Folkins et al. 2006b). This equation can be simplified to a form like Eq. (5), but with $i\sigma$ replaced by $(i\sigma + \alpha_c)$. The inclusion of this damping term [$\alpha_c \sim (4 \text{ months})^{-1}$] will change the phase relationship between A_1 and w_1 from 90° (for ozone) to approximately 65° (for CO), which equates to an approximate one month phase delay for CO compared to ozone. This is reasonably consistent with the phase behavior seen in the 68 hPa time series in Fig. 8.

Figure 9a shows the vertical profile of the relative amplitude of the CO annual cycle $(A_1/\langle A\rangle)$ derived from the 2 years of MLS data, for pressure levels 147–46 hPa. There is a strong peak in the annual cycle amplitude at the 68-hPa level (as seen in Fig. 8), and this occurs in a region where the vertical gradient of CO is large (Fig. 9b). Because of the limited vertical extent and sensitivity of the MLS data, Fig. 9b includes the vertical profile of tropical CO as derived from several other data sources (taken from Folkins et al. 2006b). Overall CO exhibits a well-mixed (relatively flat) ver-

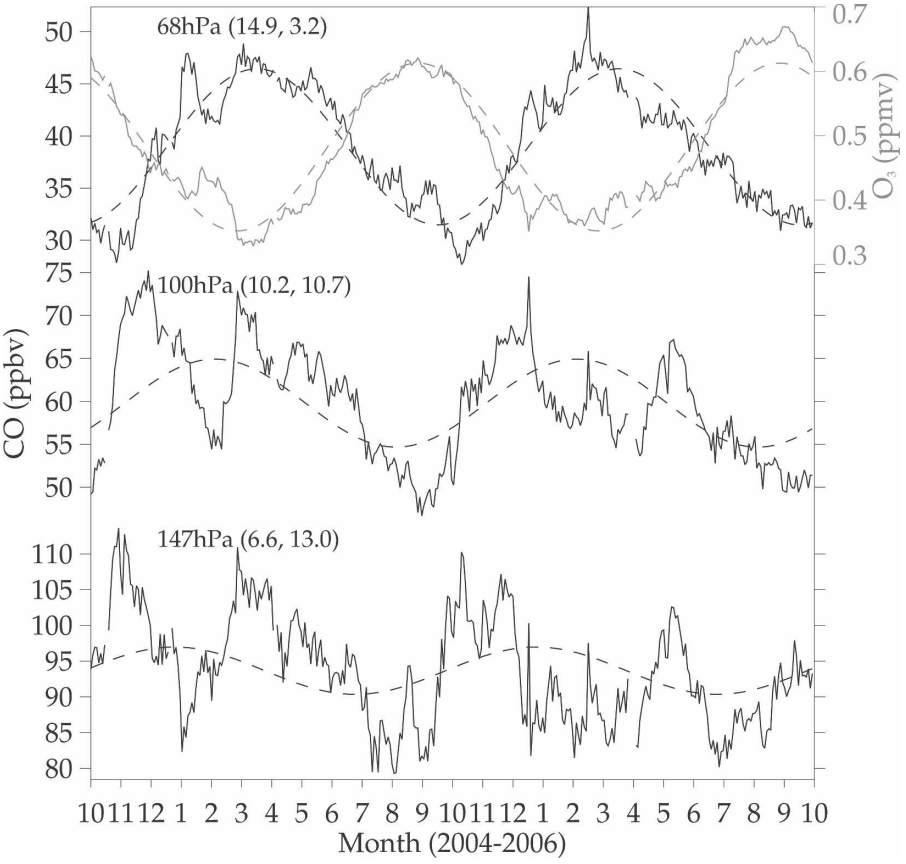

FIG. 8. Time series of MLS CO averaged over 10°S–20°N at 147, 100, and 68 hPa, for data spanning 2004–06. The dashed lines show the respective annual harmonic fits to the time series, and the amplitude of the annual and semiannual harmonics (ppmv) at each level are indicated. A corresponding time series of MLS ozone is also shown for the 68-hPa level.

tical structure throughout the troposphere up to ~14 km, and then decreases in the lower stratosphere because of photochemical loss. Note that the large annual cycle amplitude at 68 hPa occurs precisely in the region of strongest vertical gradient in the background structure (Fig. 9b). Assuming the approximate continuity equation with damping [Eq. (6)], the annual cycle amplitude in vertical velocity can be estimated as in Eq. (5), but replacing $i\sigma$ with $(i\sigma + \alpha_c)$. The corresponding amplitude of w_1 is then

$$w_1 = \sqrt{\sigma^2 + \alpha_c^2}\left(\frac{A_1}{\langle A\rangle}\Big/\frac{\partial \ln\langle A\rangle}{\partial z}\right). \qquad (7)$$

The results of this calculation using $d(\ln CO)/dz$ derived from the Atmospheric Chemistry Experiment-Fourier Transform Spectrometer (ACE-FTS) profile in Fig. 9b give an estimate for w_1 of 0.13 mm s^{-1} at the 68-hPa level, which is comparable to the other estimates of w_1 in Fig. 7. Note that the upward advection of the (smaller) annual cycle in CO below the tropopause may contribute to part of the seasonal cycle in the lower stratosphere, so that the attribution to w_1 [Eq. (7)] provides an upper limit to estimating w_1. If the ~7-ppmv annual cycle at 147 hPa propagates unattenuated to 68 hPa, then the corresponding amplitude of w_1 could be reduced by ~40%; a smaller reduction (~20%) would occur given the ~3-month propagation time and photochemical damping. We include this latter estimate of w_1 (~0.1 mm s^{-1}) in Fig. 7, showing reasonable agreement with the other results (especially given the low vertical resolution of the MLS CO data). Overall the presence of annual variations in CO below the tropopause introduces larger uncertainties in estimates of w_1 compared to the case for ozone. However, the clear increase in CO annual cycle amplitude with height together with the observed phase structure (and relation to ozone) are strong evidence that the CO annual cycle above the tropopause is primarily driven by the annual cycle in upwelling.

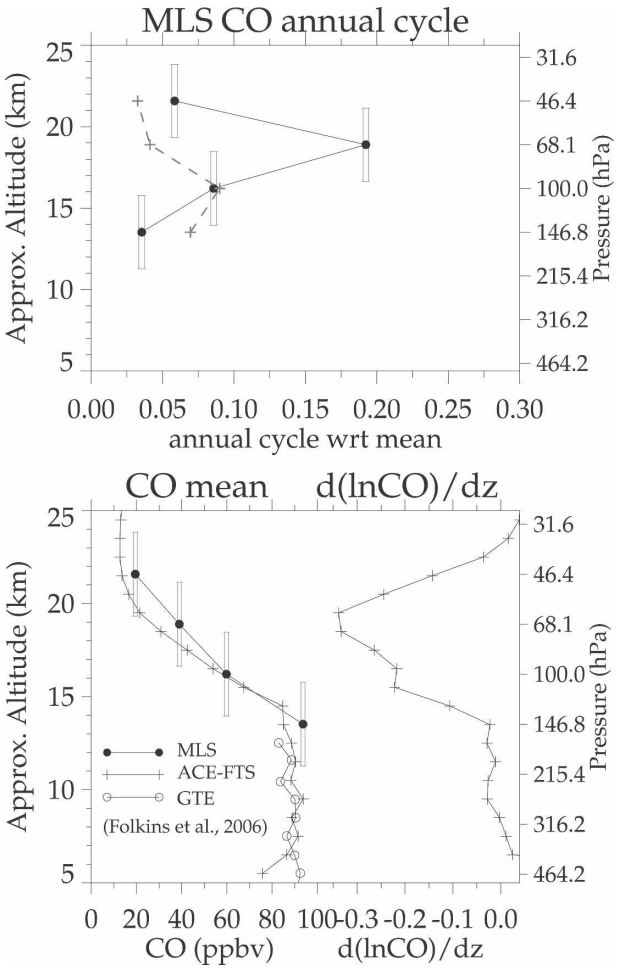

FIG. 9. (top) Relative annual cycle amplitude for CO derived from MLS data over 10°S–20°N during 2004–06. The vertical bars denote the width of the MLS sampling. The dashed line indicates the relative amplitude of the semiannual harmonic. (bottom) Vertical profile of background tropical CO mixing ratio derived from MLS data (over 147–46 hPa), together with results presented in Folkins et al. (2006b) (based on aircraft and satellite measurements). Profile on the right is the quantity $d(\ln CO)/dz$ based on ACE-FTS data (Bernath et al. 2005).

4. Summary and discussion

Ozonesonde measurements from the SHADOZ network reveal a large annual cycle in ozone near and above the tropical tropopause. The relative annual cycle amplitude is large in a relatively narrow vertical layer spanning ~16–19 km, with approximately a factor of 2 variation between maximum and minimum ozone values during the year. The large ozone annual cycle is also observed in satellite data, although measurements with reduced vertical resolution can substantially underestimate the amplitude. The ozone seasonal cycle is approximately in phase with the well-known annual cycle in temperature, and the relative ozone amplitude has a similar vertical structure to that of temperature (with a peak near 17.5 km). We have shown that the ozone annual cycle above the tropopause arises primarily because of vertical transport associated with the annual cycle in tropical upwelling. This is evidenced by the approximate quadrature phase relationship between ozone and calculated upwelling (Fig. 6), which is consistent with the approximate in-phase behavior between ozone and temperature. More importantly, this mechanism explains the detailed vertical structure of the ozone annual cycle, as the narrow vertical structure arises as a result of the strong background vertical gradient in ozone near and above the tropopause (specifically, the relative amplitude is proportional to $d\ln O_3/dz$). This background structure is fundamentally due to the rapid photochemical increase in ozone in the lower stratosphere. Hence, the similarity in vertical structure between the ozone and temperature annual cycles (Figs. 3a and 5) may be partly fortuitous, in that the temperature maximum near 17.5 km is mainly due to the long radiative relaxation time scales in this region (Randel et al. 2002), whereas the ozone maximum occurs because of the background photochemical structure. However, the radiative effect of these in-phase ozone changes will probably enhance the temperature seasonal cycle in the lower stratosphere, perhaps accounting for some substantial fraction of the observed temperature amplitude (i.e., temperature in a response to both dynamically driven upwelling and ozone radiative effects). This effect could be included as a forcing term in the simplified thermodynamic balance [Eq. (1)], and would reduce the radiative relaxation time scales in this region deduced from dynamical upwelling in Randel et al. (2002). Note this influence of ozone on temperature is consistent with the results of Folkins et al. (2006a), who demonstrate that tropical upwelling calculated from observed temperature variations is reduced if the radiative effects of ozone are included (or in other words, the temperature seasonal cycle associated with dynamical upwelling is smaller than the observed variation).

The simplified ozone continuity equation [Eq. (5)] provides a relation between the observed ozone variability and the annual cycle in tropical upwelling, and we have used this to estimate the vertical structure and magnitude of w_1. The results in Fig. 6 show reasonable agreement between w_1 calculated from detailed thermodynamic balance and that derived from ozone, and we view this agreement as further evidence that the simplified continuity equation represents a reasonable approximation for ozone in the tropical lower stratosphere.

While the SHADOZ observations show a consistent annual cycle among the different stations above ~16 km (spanning a range of longitudes), there is less consistency for the annual cycle below 15 km (Fig. 3a). This behavior probably results from the strong local influence of ozone (and ozone precursor) sources in the upper troposphere, related to the well-known ozone maximum in the tropical Atlantic region (Thompson et al. 2003b; Edwards et al. 2003). While the influence of tropical deep convection will likely play some role in the seasonal cycle over convectively active regions (Folkins et al. 2006a), the evidence here suggests that the coherent annual cycle above 16 km primarily results from the annual cycle in zonal mean upwelling (which is linked to large-scale wave forcing in both the Tropics and extratropics; e.g., Yulaeva et al. 1994; Kerr-Munslow and Norton 2006; Dima and Wallace 2007).

Prompted by the analysis of Folkins et al. (2006a), we have examined the annual cycle of carbon monoxide (CO) as observed in MLS satellite data. Time series of data spanning 2 years show a strong annual cycle in CO in the lower stratosphere, with a maximum relative amplitude near 68 hPa. The CO annual cycle at 68 hPa is approximately out of phase with the ozone (and temperature) annual cycle, and this is consistent with the oppositely signed vertical gradient in CO in the tropical lower stratosphere. The maximum relative amplitude in CO occurs near the same altitude as the maximum in $d(\ln CO)/dz$ (Fig. 9), consistent with the approximate continuity equation given by (6). Overall the space–time characteristics of the CO annual cycle are consistent with forcing by the seasonal variation in upwelling, acting on the strong background vertical gradient in CO (which is related to photochemical destruction of CO above the tropopause).

We note that this interpretation of the CO annual cycle in the tropical lower stratosphere is somewhat different from the "tape recorder" signal discussed in Schoeberl et al. (2006). The tape recorder signal is based on vertical advection of relative CO extrema in the upper troposphere into the lower stratosphere by the mean upwelling circulation (which may or may not have a seasonal variation). This mechanism is distinct from a constituent seasonal cycle induced by the seasonal cycle in upwelling acting on the background vertical gradient in CO. MLS data (Figs. 8–9a) show that a semiannual variation dominates tropical CO near and below the tropopause (associated with tropospheric CO sources), whereas the annual cycle amplitude increases strongly above the tropopause. This is strong evidence that stratospheric CO variability arises primarily from the seasonal cycle in tropical upwelling, rather than from advection of the seasonal variation of CO in the upper troposphere.

Acknowledgments. We thank Qiang Fu for providing the radiative heating code used in the thermodynamic upwelling calculations. J.-F. Lamarque and Rolando Garcia provided helpful discussions and comments on the manuscript. This work is partially supported under the NASA ACMAP program.

REFERENCES

Andrews, D. G., J. R. Holton, and C. B. Leovy, 1987: *Middle Atmosphere Dynamics*. Academic Press, 489 pp.

Avalone, L. M., and M. J. Prather, 1996: Photochemical evolution of ozone in the lower tropical stratosphere. *J. Geophys. Res.,* **101,** 1457–1461.

Bernath, P. F., and Coauthors, 2005: Atmospheric Chemistry Experiment (ACE): Mission overview. *Geophys. Res. Lett.,* **32,** L15S01, doi:10.1029/2005GL022386.

Corti, T., B. P. Luo, Q. Fu, H. Vomel, and T. Peter, 2006: The impact of cirrus clouds on tropical troposphere-to-stratosphere transport. *Atmos. Chem. Phys.,* **6,** 2539–2547.

Dima, I. M., and J. M. Wallace, 2007: Structure of the annual-mean equatorial planetary waves in the ERA-40 reanalyses. *J. Atmos. Sci.,* **64,** 2862–2880.

Edwards, D. P., and Coauthors, 2003: Tropospheric ozone over the tropical Atlantic: A satellite perspective. *J. Geophys. Res.,* **108,** 4237, doi:10.1029/2002JD002927.

Folkins, I., P. Bernath, C. Boone, G. Lesins, N. Livesey, A. M. Thompson, K. Walker, and J. C. Witte, 2006a: Seasonal cycles of O3, CO, and convective outflow at the tropical tropopause. *Geophys. Res. Lett.,* **33,** L16802, doi:10.1029/2006GL026602.

——, and Coauthors, 2006b: Testing convective parameterizations with tropical measurements of HNO_3, CO, H_2O, and O_3: Implications for the water vapor budget. *J. Geophys. Res.,* **111,** D23304, doi:10.1029/2006JD007325.

Fueglistaler, S., and Q. Fu, 2006: Impact of clouds on radiative heating rates in the tropical lower stratosphere. *J. Geophys. Res.,* **111,** D23202, doi:10.1029/2006JD007273.

Kerr-Munslow, A. M., and W. A. Norton, 2006: Tropical wave driving of the annual cycle in tropical tropopause temperatures. Part I: ECMWF analyses. *J. Atmos. Sci.,* **63,** 1410–1419.

Logan, J. A., 1999: An analysis of ozonesonde data for the lower stratosphere: Recommendations for testing models. *J. Geophys. Res.,* **104,** 16 151–16 170.

McCormick, M. P., J. M. Zawodny, R. E. Veiga, J. C. Larson, and P. H. Wang, 1989: An overview of SAGE I and II measurements. *Planet. Space Sci.,* **37,** 1567–1586.

Pan, L., S. Solomon, W. Randel, J.-F. Lamarque, P. Hess, J. Gille, E.-W. Chiou, and M. P. McCormick, 1997: Hemispheric asymmetries and seasonal variations of the lowermost stratosphere water vapor and ozone derived from SAGE II data. *J. Geophys. Res.,* **102,** 28 177–28 184.

Plumb, R. A., and J. Eluszkiewicz, 1999: The Brewer–Dobson circulation: Dynamics of the tropical upwelling. *J. Atmos. Sci.,* **56,** 868–890.

Randel, W. J., R. R. Garcia, and F. Wu, 2002: Time-dependent upwelling in the tropical lower stratosphere estimated from

the zonal-mean momentum budget. *J. Atmos. Sci.,* **59,** 2141–2152.

——, F. Wu, and W. Rivera Ríos, 2003: Thermal variability of the tropical tropopause region derived from GPS/MET observations. *J. Geophys. Res.,* **108,** 4024, doi:10.1029/2002JD002595.

——, ——, H. Vömel, G. E. Nedoluha, and P. Forster, 2006: Decreases in stratospheric water vapor after 2001: Links to changes in the tropical tropopause and the Brewer-Dobson circulation. *J. Geophys. Res.,* **111,** D12312, doi:10.1029/2005JD006744.

Reed, R. J., and C. L. Vlcek, 1969: The annual temperature variation in the lower tropical stratosphere. *J. Atmos. Sci.,* **26,** 163–167.

Rosenlof, K. H., 1995: Seasonal cycle of the residual mean meridional circulation in the stratosphere. *J. Geophys. Res.,* **100,** 5173–5191.

Russell, J. M., III, A. F. Tuck, L. L. Gordley, J. H. Park, S. R. Drayson, J. E. Harries, R. J. Cicerone, and P. J. Crutzen, 1993: The HALOGEN Occultation Experiment. *J. Geophys. Res.,* **98,** 10 777–10 797.

Schoeberl, M. R., B. N. Duncan, A. R. Douglass, J. Waters, N. Livesey, W. Read, and M. Filipiak, 2006: The carbon monoxide tape recorder. *Geophys. Res. Lett.,* **33,** L12811, doi:10.1029/2006GL026178.

Thompson, A. M., and Coauthors, 2003a: Southern Hemisphere Additional Ozonesondes (SHADOZ) 1998–2000 tropical ozone climatology. 1. Comparison with Total Ozone Mapping Spectrometer (TOMS) and ground-based measurements. *J. Geophys. Res.,* **108,** 8238, doi:10.1029/2001JD000967.

——, and Coauthors, 2003b: Southern Hemisphere Additional Ozonesondes (SHADOZ) 1998–2000 tropical ozone climatology. 2. Tropospheric variability and the zonal wave-one. *J. Geophys. Res.,* **108,** 8241, doi:10.1029/2002JD002241.

Uppala, S. M., and Coauthors, 2005: The ERA40 Reanalysis. *Quart. J. Roy. Meteor. Soc.,* **131,** 2961–3012.

Volk, C. M., and Coauthors, 1996: Quantifying transport between the tropical and midlatitude lower stratosphere. *Science,* **272,** 1763–1768.

Waters, J., and Coauthors, 2006: The Earth Observing System Microwave Limb Sounder (EOS MLS) on the Aura satellite. *IEEE Trans. Geosci. Remote Sens.,* **44,** 1075–1092.

Wickert, J., and Coauthors, 2001: Atmosphere sounding by GPS radio occultation: First results from CHAMP. *Geophys. Res. Lett.,* **28,** 3263–3266.

Yulaeva, E., J. R. Holton, and J. M. Wallace, 1994: On the cause of the annual cycle in tropical lower stratosphere temperatures. *J. Atmos. Sci.,* **51,** 169–174.